Multispacecraft current estimates at swarm

Dunlop, M. W.; Yang, Y.-Y.; Yang, J.-Y.; Lühr, H.; Shen, C.; Olsen, Nils; Ritter, P.; Zhang, Q.-H.; Cao, J.-B.; Fu, H.-S.; Haagmans, R.

Published in:
Journal of Geophysical Research: Space Physics

Link to article, DOI:
10.1002/2015ja021707

Publication date:
2015

Document Version
Publisher's PDF, also known as Version of record

AGU PUBLICATIONS

JGR

Journal of Geophysical Research: Space Physics

RESEARCH ARTICLE
10.1002/2015JA021707

Key Points:
- Two-, three-, and four-point analyses of electric currents at low Earth orbit
- Comparative analysis of field-aligned current density: test of stability
- Direct measure of perpendicular currents in the upper ionosphere for the first time

Correspondence to:
M. W. Dunlop,
m.w.dunlop@rl.ac.uk

Citation:
Dunlop, M. W., et al. (2015), Multispacecraft current estimates at swarm, *J. Geophys. Res. Space Physics*, *120*, 8307–8316, doi:10.1002/2015JA021707.

Received 21 JUL 2015
Accepted 28 AUG 2015
Accepted article online 5 SEP 2015
Published online 3 OCT 2015

Multispacecraft current estimates at swarm

M. W. Dunlop[1,2], Y.-Y. Yang[3], J.-Y. Yang[1], H. Lühr[4], C. Shen[5], N. Olsen[6], P. Ritter[5], Q.-H. Zhang[7], J.-B. Cao[1], H.-S. Fu[1], and R. Haagmans[8]

[1]Space Science Institute, School of Astronautics, Beihang University, Beijing, China, [2]RAL, Didcot, UK, [3]The Institute of Crustal Dynamics, CEA, Beijing, China, [4]GFZ, Potsdam, Germany, [5]NSSC, CAS, Beijing, China, [6]DTU Space, Lyngby, Denmark, [7]CSW, Institute of Space Sciences, Shangdong University, Weihai, China, [8]ESA/ESTEC, Noordwijk, Netherlands

Abstract During the first several months of the three-spacecraft Swarm mission all three spacecraft came repeatedly into close alignment, providing an ideal opportunity for validating the proposed dual-spacecraft method for estimating current density from the Swarm magnetic field data. Two of the Swarm spacecraft regularly fly side-by-side in closely similar orbits, while the third at times approaches the other two. This provides a data set which under certain assumptions of stationarity of the magnetic field can produce 2, 3, 4, 5 (or more) point measurements, which can be cross compared. We find that at low Earth orbit the use of time-shifted positions allow stable estimates of current density to be made and can verify temporal effects as well as validating the interpretation of the current components as arising predominantly from field-aligned currents. In the case of four-spacecraft configurations we can resolve the full vector current and therefore can check the perpendicular as well as parallel current density components directly, together with the quality factor for the estimates directly (for the first time in situ at low Earth orbit).

1. Introduction

The curlometer technique [*Dunlop et al.*, 1988, 2002] and its derivatives have been established over the last decade or so as a key method of estimating the electric current density in a number of regions of the magnetosphere. More generalized methods estimating the curvature and gradient of the magnetic field have also been extensively applied to multispacecraft magnetic field measurements [*Shen et al.*, 2007, 2012a, 2012b; *Vogt et al.*, 2009] from both Cluster and Time History of Events and Macroscale Interactions during Substorms (THEMIS) [e.g., *Dunlop et al.*, 2002; *Shen et al.*, 2012a, 2012b]. Although these methods have been predominantly applied to the outer magnetospheric regions (dayside magnetopause, magnetotail, and lobes), where the influence of the Earth's internal field is weak and temporal fluctuations are often dominant, recently, there have been a number of studies using multispacecraft estimates of current density in the inner magnetospheric regions and ring current [*Vallat et al.*, 2005; *Zhang et al.*, 2011; *Shen et al.*, 2014] and in regions supporting field-aligned currents [*Marchaudon et al.*, 2009; *Shi et al.*, 2010, 2012]. In order to better disentangle the temporal and spatial variations in the magnetosphere, the multispacecraft techniques are generally applied as purely spatial estimates, point by point in time. In low Earth regions of the magnetosphere, however, studies have until now relied on estimates arising from single-spacecraft data, for which the disentangling of temporal and spatial variations is difficult [*Lühr et al.*, 2015], and have focused on large- or small-scale field-aligned currents (FACs) and the modeling of signals associated with the external influences in the geomagnetic field (e.g., the ring current).

The advent of the three-spacecraft Swarm mission (labelled A, B, and C) has provided the opportunity to perform direct estimates of current density through multispacecraft techniques, removing at least some of the ambiguity arising from single-spacecraft methods. The Swarm [*Friis-Christensen et al.*, 2008] spacecraft are flying in circular, polar, low Earth orbits (LEOs). They were launched on 22 November 2013 and underwent a sequence of maneuvers to adjust the phasing of each of the three spacecraft. After 17 April 2014, a final configuration was achieved for which A and C fly side-by-side (the separation is ~100–150 km), at a mean altitude of about 481 km and an orbital period of ~94 min, while Swarm B is flying at a slightly higher orbit of ~531 km, with a slightly different orbital period of ~95 min [see *Dunlop et al.*, 2015]. Swarm B was initially aligned with the orbital planes of A and C so that at the start of science operations all orbit planes were closely aligned and the three spacecraft flew close to each other at times, where this close configuration repeats every few days. The polar orbits take the Swarm spacecraft through the auroral regions and across the polar cap at high latitudes and sample all local times in about 132 days (spacecraft A/C), similar to the coverage of the CHAMP spacecraft [*Reigber et al.*, 2002].

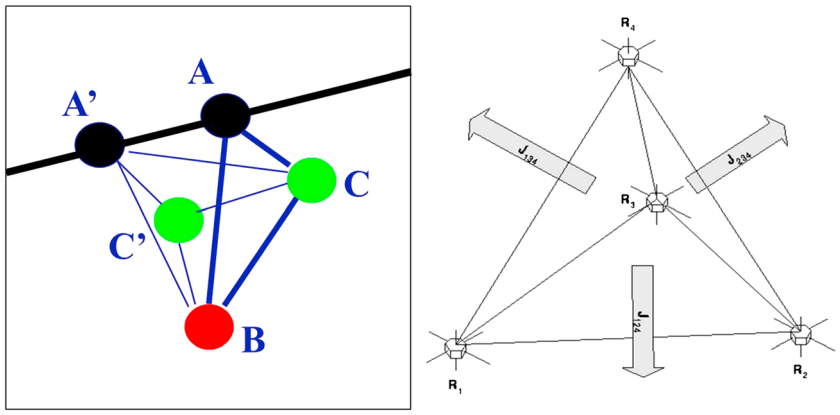

Figure 1. Illustration of the multispacecraft technique as applied to Swarm measurements, where the left plot is as shown in *Dunlop et al*. [2015] and is described there, i.e., "the three Swarm spacecraft, A, B, and C, are drawn relative to the orbit of Swarm A for a particular time. The positions A′ and C′ are drawn for their positions at a slightly earlier time. For nominal operations, the spacecraft A and C fly side-by-side along similar orbits having slightly different local times (which crossover as the spacecraft fly over the poles). Swarm B is flying at a slightly higher altitude and in this example lags behind the A-C pair. The picture on the right is from *Dunlop et al*. [1988] and depicts the estimate of average current normal to each face of the tetrahedron formed by four positions. The current for the back face is not shown.

Here we apply the methodology of the curlometer technique to the close configurations of Swarm to achieve 3- and 4-point estimates of electric current density, and using combinations of spacecraft positions we test the temporal stability and the validity of inferring the field-aligned component from time-shifted spacecraft positions (extending the work of *Ritter and Lühr* [2006] and *Ritter et al*. [2013]).

2. Methodology

A phased array of spacecraft in principle allows spatial gradient estimates of magnetic field measurements (in particular) to be made. For example, the four Cluster spacecraft, flying in formation, provide four spatial positions from which a direct calculation of the curl of the magnetic field can be made, thereby providing an estimate of all components of the electric current density [*Dunlop et al*., 1988, 2002; *Robert et al*., 1998]. This is shown schematically on the right-hand side of Figure 1, where the spacecraft configuration affects the quality of the estimate. The curlometer estimate is based on the assumption that curl(**B**) = $\mu_0 J$ (i.e., using Ampère's law to estimate the average current density through the tetrahedron) and using the qualifying parameter div**B** = 0. The linear, integral form of Ampère's law estimates the average current, J, normal to the face 1_{ij} of the tetrahedron from

$$\mu_0 < J > \left(\Delta r_i \Delta R_j\right) = \Delta B_i \cdot \Delta R_j - \Delta B_j \cdot \Delta R_i, \quad \text{e.g.,} \ \mu_0 < J >_{123} \left(\Delta r_{12} \Delta R_{13}\right) = \Delta B_{12} \cdot \Delta R_{13} - \Delta B_{13} \cdot \Delta R_{12}$$

We also have

$$< \mathrm{div}(B) > \left|\Delta R_i \cdot \Delta R_j \Delta R_k\right| = \left|\Sigma_{\mathrm{cyclic}} \Delta B_i \cdot \Delta R_j \Delta R_k\right|$$

i.e., $<\mathrm{div}(B)>_{1234}(\Delta R_{12} \cdot \Delta R_{13} \wedge \Delta R_{14}) = \Delta B_{12} \cdot \Delta R_{13} \wedge \Delta R_{14} + \Delta B_{13} \cdot \Delta R_{14} \wedge \Delta R_{12} + \Delta B_{14} \cdot \Delta R_{12} \wedge \Delta R_{13}$, which provides an indirect quality indicator of the neglected nonlinear gradients [*Dunlop et al*., 2002; *Robert et al*., 1998].

In these equations, ΔB_{ij} and ΔR_{ij} represent the vector difference in the measured magnetic field vector and spatial position vector of the spacecraft labelled i and j, respectively. There is also a redundancy in the estimate, since the vector current can be constructed from three of the faces of the tetrahedron, and this can be used to verify the sensitivity of the estimate for each component of J. If only three spacecraft are used in the calculation (for example, if the spacecraft configuration is severely distorted), then only the current component, J_N, normal to the corresponding face of the tetrahedron is obtained. The other components are then not estimated, so that the significance of the calculation depends on the alignment of the normal to the magnetic structures. For example, in the case of Cluster or THEMIS, typically, in the in situ ring current, the azimuthal ring current component, J_ϕ, is reliably returned [*Zhang et al*., 2011; Y. Y. Yang et al., Storm time current distribution in the inner magnetospheric equator: THEMIS observations, submitted to *Journal of Geophysical Research, Space Physics*, 2015] since the configuration often aligns perpendicularly to the ring plane. Also, in the case of FACs,

the alignment of J_N to $J_{||}$ is significant. Thus, previous experience with Cluster measurements has shown that regular configurations of the spacecraft (as well as the comparative scale size) are optimal [*Dunlop et al.*, 2002; *Robert et al.*, 1998], while distorted tetrahedral configurations return stable components only for particular alignments with magnetic structure.

The three Swarm spacecraft (named A, B, and C), even when flying in close formation, allow only a partial estimate of the current density (i.e., one component, normal to the plane of the configuration) unless assumptions are made about the stationarity of the magnetic field at LEO. At these low Earth altitudes, the internal geomagnetic field, which contains nonlinear gradients, dominates, so that linear estimators of the currents should be applied to the residual field, obtained following subtraction of the static internal field in order to remove errors introduced by the neglect of the nonlinear terms (this is also true for estimates performed in the near ring current at ~3–7 R_E [e.g., *Shen et al.*, 2014]). Furthermore, temporal variations are often slower than the sampling rate of magnetic structures at LEO, so that the field structure can be considered to be stationary for short time periods and adjacent positions of the spacecraft in time can be considered to sample the same current structure, thereby providing additional spatial positions. In particular, if the spatial structure of the magnetic field is assumed to be stationary on short time scales of a few up to 20 s, and is suitably filtered, then adjacent (time-shifted) positions of the spacecraft can add to the number of spatial positions used to estimate the differences in the magnetic field between each position. In Figure 1, for example, the magnetic field values at the positions of spacecraft A and C at earlier or later times (typically shifted by 5–20 s to regularize the configuration) can be combined with the positions of the A, B, and C spacecraft at some time, to provide a measurement set of up to 5 spatial points, from which the magnetic gradients (and curl**B** in particular) may be estimated. Other configurations result if the position of B is also time shifted.

Ritter and Lühr [2006] applied this technique to the A-C lower-altitude pair of Swarm spacecraft flying side-by-side. Here we extend the method in the sense of the possible configurations in Figure 1 obtained by selecting different sets of positions, to produce two-, three-, and four-spacecraft estimates of current density from the basic three-spacecraft spatial configuration of Swarm. By selecting groups of three or four spacecraft (as well as using the spatial array ABC), a "curlometer" estimate can be made such that three-spacecraft positions essentially form one face of the tetrahedron shown in the right-hand plot of Figure 1 (the use of four-spacecraft positions recover the full curlometer estimate). In order to get four (or more) spacecraft we can introduce additional "virtual" spacecraft by time shifting the three spacecraft A, B, and C. Here we form a basic array by conceptually time shifting spacecraft A and C. There are, in fact, four sets of four spacecraft, involving spacecraft B, as drawn in Figure 1, that can be formed from the five positions shown (the array AA'CC' is nearly planar so it is not a usable fifth grouping; see below). In the case of four spacecraft the quality parameter from the linear estimate of div**B**/curl**B** can also be estimated [*Dunlop et al.*, 1988]. The curlometer estimate provides a stable result point-by-point in time, and an indirect measure of the quality of the four-spacecraft estimate can therefore be tracked by div**B**/curl**B**, for example, with the stability being monitored by different selections of spacecraft positions. Thus, if three Swarm spacecraft are close together, as shown here, different tetrahedral configurations may be selected so that the five positions provide some redundancy in the calculation, allowing the quality of the estimate to be tested.

Nevertheless, a number of points should be noted. First, time shifting AC results in a nearly planar configuration of four positions (AA'CC'), where only one component of the current density is found so that the field-aligned current in particular is only obtained from a projection onto the field-aligned direction of the component normal to the spacecraft plane containing the spacecraft positions. This is true for the standard "dual-satellite" level 2 (L2) data product FAC_TMS_2F in the Swarm data set, calculated from the two spacecraft (A and C), time-shifted method [*Ritter et al.*, 2013]. Second, the current density estimate resulting from each group of spacecraft relates to a particular barycenter (center of volume of the configuration [see *Harvey*, 1998]), so that the combination of different groups of spacecraft refers to slightly different times. This allows the degree of stationarity of the measurement to be probed, in principle, through different choices of spacecraft (which results in different mean times for the corresponding barycenter). For example, three-spacecraft combinations (such as ACC' and AA'C) can be selected and refer to slightly different mean times. For the special case of the configuration in Figure 1, both four- and three-spacecraft estimates can be cross compared. The combination of Swarm A, B, and C produces a purely spatial estimate, but is typically in a slightly tilted plane to the A, C orbit tracks and additionally corresponds to the leading time of measurement. We have chosen to show results below from the configurations formed through time shifting the positions of A and C (as indicated in Figure 1), since this produces

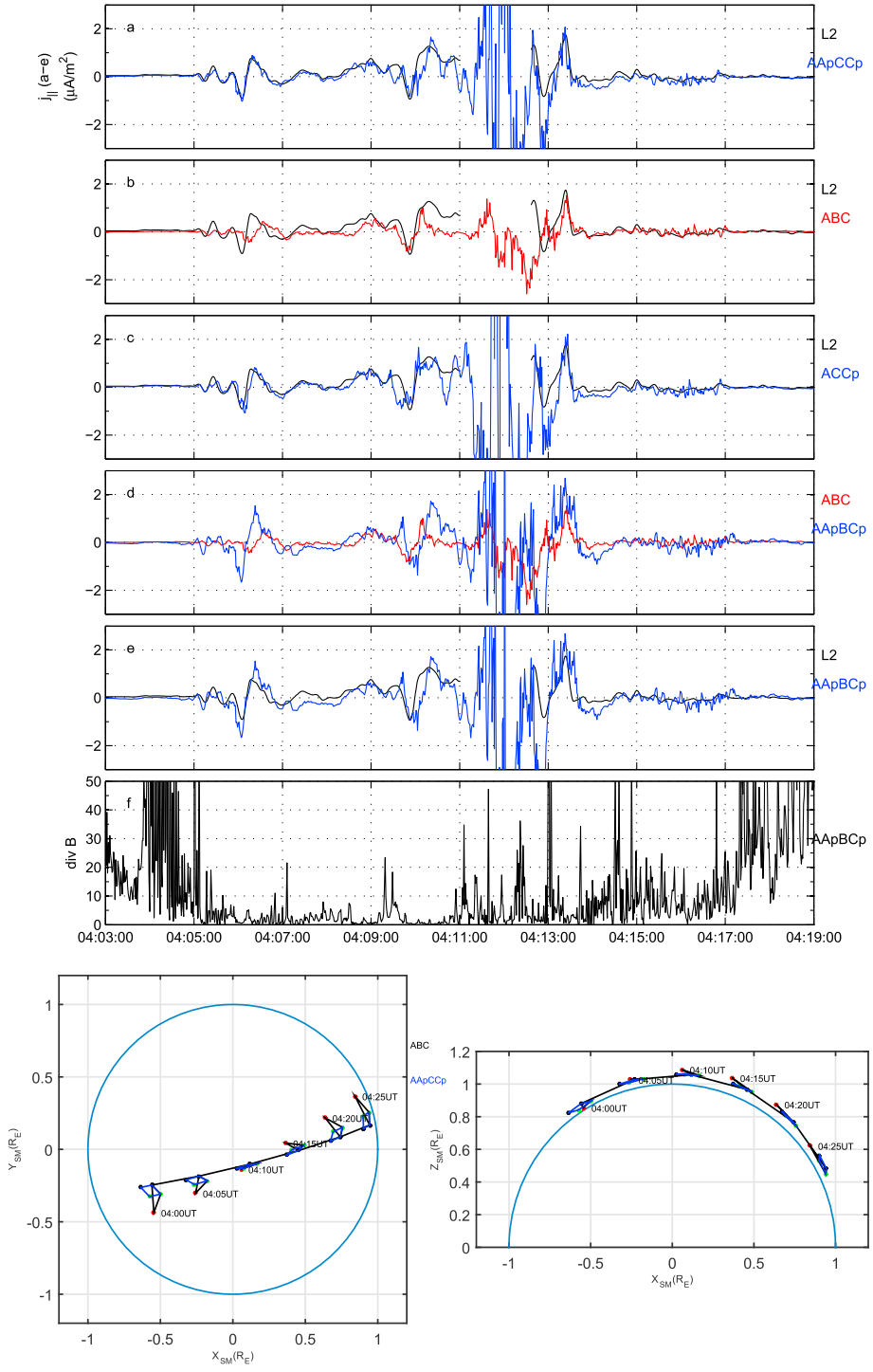

Figure 2. A set of curlometer comparisons, for the data collected during 22 April 2014: (top, a) the unsmoothed estimate using positions AApCCp, compared to the smoothed level 2 (L2) data product; (b) the three-spacecraft spatial array, using ABC (i.e., no time shift, pure gradient calculation, which has a different J_N direction), compared to the L2 estimate; (c) 3-point formation, ACCp, compared to the L2 estimate; (d) comparison of the 4-point array (AApBCp) with the (e) ABC and L2 estimates, respectively; and (f) the ratios of div**B**/curl**B** (labelled div**B** for short) for the 4-point estimate. (bottom) The orbit views ((right) X-Y_{SM} and (left) X-Z_{SM}) show enlarged (5X) configurations as the Swarm spacecraft flew over the auroral zone and polar cap.

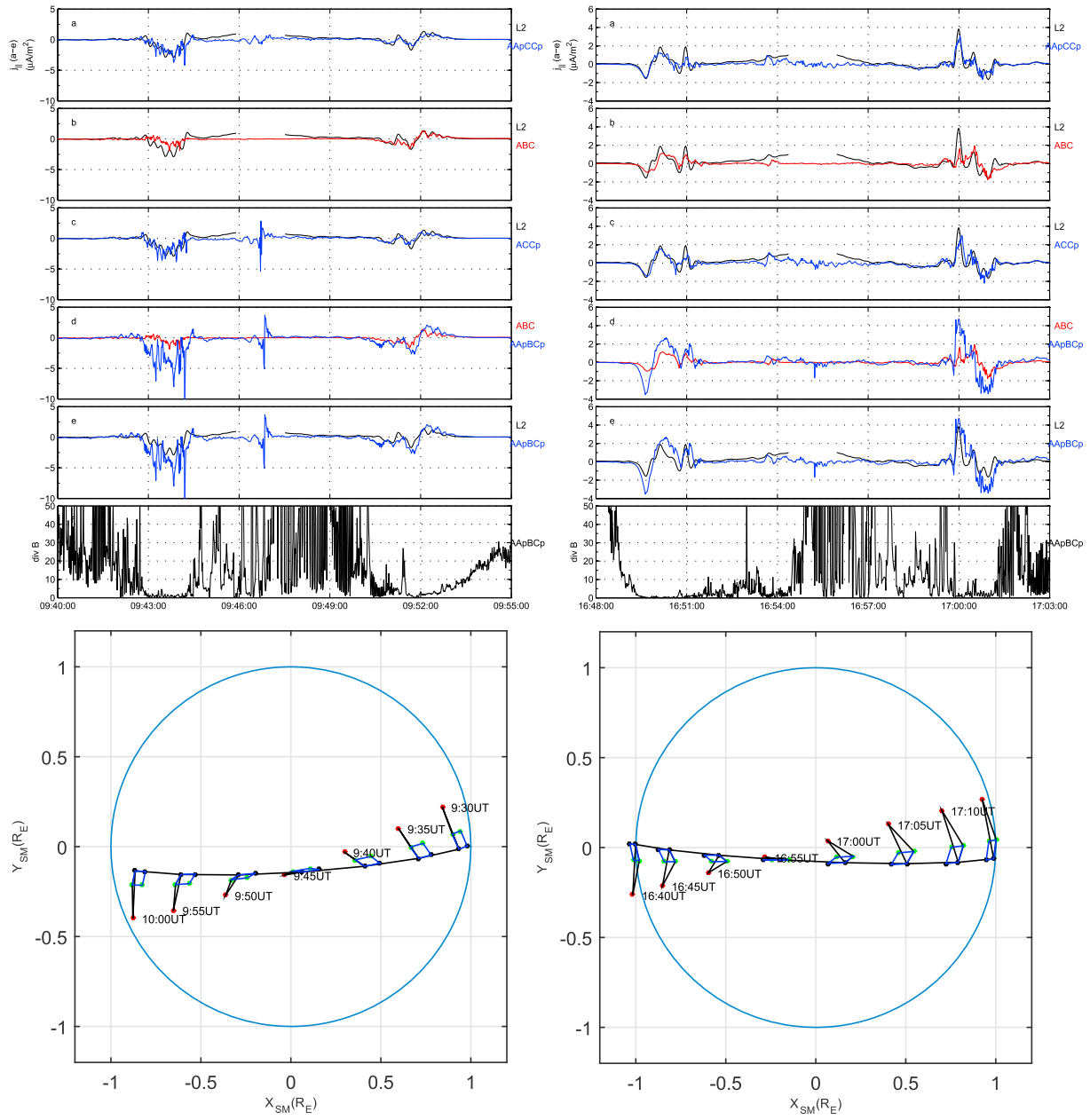

Figure 3. Set of curlometer comparisons in the same format as Figure 2, with the X-Y_{SM} projections of the configurations, including time-shifted positions, shown in the bottom plots. The left-hand plots correspond to the pass on the 28 April 2014 and the right-hand plot to the 4 May 2014.

the best alignment of the configurations to the L2 two-spacecraft parameter, and of course, we expect that in this high-latitude region the dominant currents will be field aligned and therefore approximately perpendicular to the basic plane formed by AA'CC'. The alignment is less critical for the four-spacecraft estimates, but it is still useful to use this choice for the L2 comparisons (see later discussion). We note, however, that a more generalized method of constructing (or measuring) the configuration can be devised, as studied in terms of homogeneity scales in the least squares approach discussed by *De Keyser* [2008] (and see references therein), and this could be used in future applications and compared to other gradient methods (see Conclusions). Here we benefit from the special context of the Swarm orbit geometry and natural alignment expected of the main FACs.

It is therefore instructive to compare the estimates found from different combinations, and below we show the comparison of the various estimates for a number of events.

3. Event Tests

In order to test the application of the curlometer to the Swarm data we select events from the first phase of science operations (April–August 2014), when the alignment of the orbits allowed the three spacecraft to repeatedly come close together. We have used 1 Hz Swarm level 1b data (https://earth.esa.int/web/guest/swarm/data-access), corrected to version 04, taken by the vector field magnetometers (VFMs) [*Friis-Christensen et al*., 2008], but where these data have had the Earth's static, internal field removed using the CHAOS-4plus model [e.g., *Olsen et al*., 2014]. The curlometer method is then applied to the residual field data.

We have adopted the labelling that the time-shifted positions, A′ and C′, are labelled such that A′ = An (for forward shift in time) or Ap (for backward shift in time) and similarly for C′ (we find that the optimum time is 20 s to best match all methods and optimally regularize the spatial configuration of the spacecraft, as is shown in Figure 1 and on the spacecraft orbits in Figures 2 and 3). We have compared the multispacecraft, curlometer estimates to the two-spacecraft, time-shifted method of *Ritter et al*. [2013] (using the Swarm level 2 product FAC_TMS_2F, derived using VFM measurements), highlighting both compatibility with this method and differences observed. The basic set of comparisons are shown in Figure 2, for the first event, where we compare the field-aligned current component in each case, first for the unsmoothed estimate arising from AApCCp, then for the different spacecraft groups defined by the enlarged constellations on the right-hand side of Figure 2. The $J_{||}$ component is taken from the projection of J_N in each 3-point case (so depends on the actual orientation of the plane of the configuration) and is the field-aligned component of the vector current in the case of the 4-point arrays. The first FAC signature in Figure 2 has been analyzed recently by *Dunlop et al*. [2015].

Figure 2a of the top plot shows that AApCCp (which are aligned to the spacecraft tracks and therefore effectively lie in a plane) fit rather well to the signature obtained from the standard L2 two-spacecraft product. The line for L2 is broken for the interval 04:11–04:12:30 UT, indicating where the orbits crossover (first spacecraft B and then AC, as indicated in the right-hand orbit plots). During this short interval, we expect the quality of the estimates to be downgraded as the form of the spacecraft array changes dramatically which is reflected in the deviations between the curves (a measure of quality) as this interval is approached from either side and by the noisiness of the estimates within the interval. Nevertheless, at other times, the profiles match in amplitude and timing throughout the interval shown, as expected for the matched orientation of the planes of the spacecraft positions. Changing the time shift has more effect between 04:10–04:11 UT and 04:12:30–04:14 UT. Figure 2b shows that the tilt of the ABC plane (as seen in the X-Z_{SM} projection in Figure 2) initially results in a lower-amplitude FAC signal since the projection of J_N is more misaligned to $J_{||}$, for this configuration. (Note that the ABC estimate is a purely spatial estimate which changes the sampling of the FAC slightly.) These effects again change through the interval as the ABC configuration changes. Figure 2c shows that the use of only three positions, ACCp, in fact also compares well with the L2 FAC signatures, although additional features are apparent. This estimate is sensitive to the choice of spacecraft positions and in principle allows the quality of the L2 FAC estimate to be verified; i.e., different choices for the three positions result in slightly different barycenter times relative to those of the L2 product, so that small temporal and spatial effects can be revealed in principle.

Figures 2e and 2f show that the full curlometer estimate, arising from a 4-point array (here chosen as AApBCp), identifies the field-aligned signatures seen in the profile of the L2 product. In addition, the time shifts in signature seen in the ABC estimate are confirmed to arise from that choice of configuration. The actual profile obtained is sensitive to the choice of spacecraft positions and the resulting configuration. This provides a further quality measure on the features observed, through the change in effective barycenter and different tetrahedral shapes formed by each four-position set. In principle, this can also be used to explore any effects of nonstationarity. For this event however, the profiles are broadly consistent. The $J_{||}$ component in this case is actually obtained from the three vector components of current density (see section 4) and so can be used even when the FAC direction deviates far from the plane of the spacecraft configurations. In fact, in both Figures 2e and 2f, this estimate produces the highest-amplitude FAC signal, suggesting that the L2 estimate (and that from the other three-spacecraft arrays) omits some of the actual FAC through the misalignment of J_N to the field-aligned direction (see section 4). The four-spacecraft estimate, despite incorporating two time-shifted positions, is in fact rather stable throughout the intervals tested and adjacent to the orbit crossovers in particular. It therefore provides additional coverage of signatures when the L2 product has low quality.

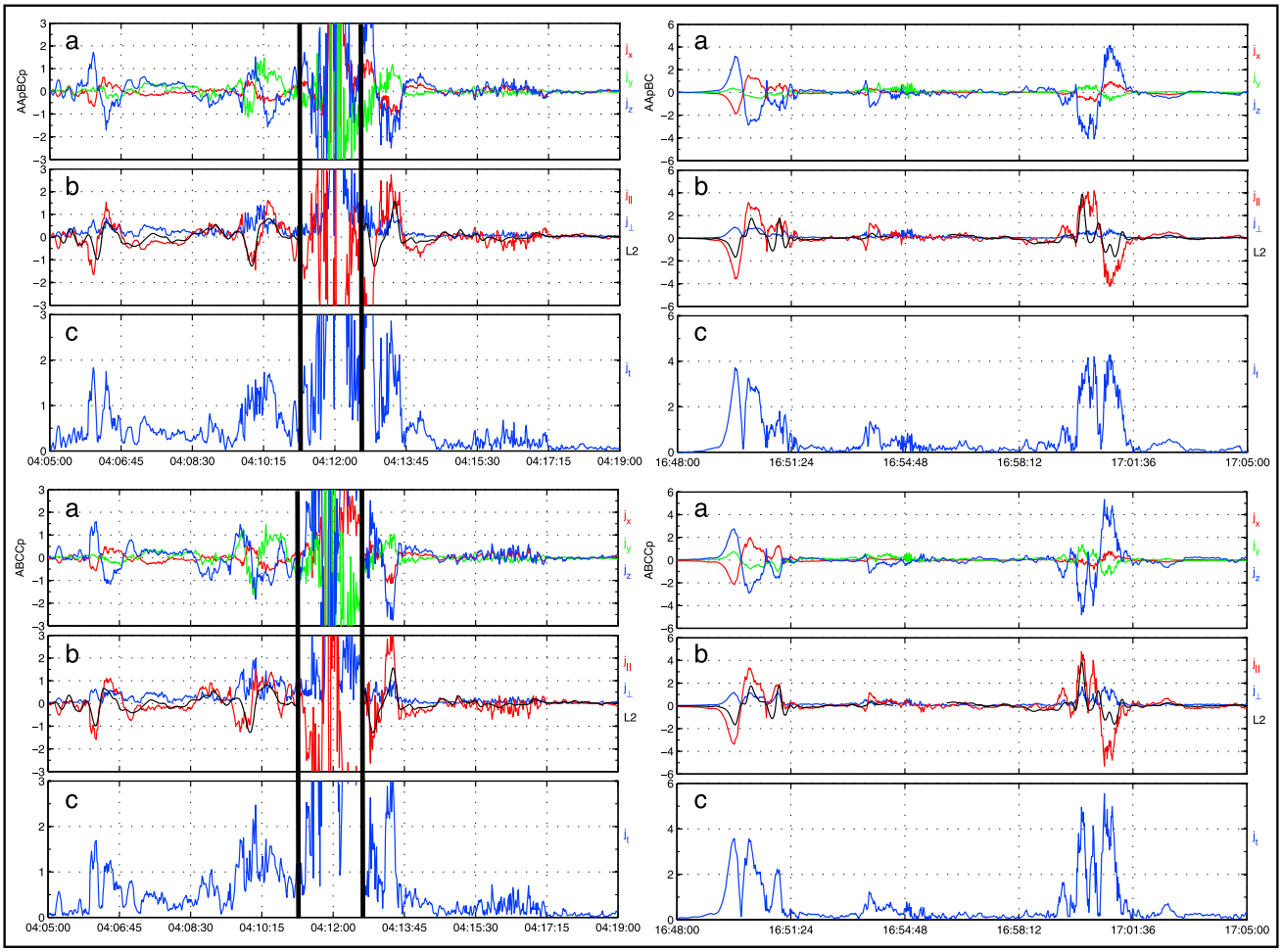

Figure 4. Vector current density estimates obtained from the 4-point estimates for the key intervals during the 22 April (left) and 4 May (right) passes. For each event we plot the estimates from two configuration choices (top and bottom plots). For each plot, the top traces show the three SM components of the vector current; the middle traces show $J_{||}$ and $J_{\boxtimes}$, together with the L2 trace; and the bottom trace shows $|J|$. The estimates for the 22 April (left-hand plots) near the orbit crossover of Swarm A/C and B (between the vertical black lines) are unreliable due to distortion of the spacecraft configuration.

Figure 2 (bottom) actually shows the standard estimate of div**B**/curl**B**, which is obtainable for each choice of four positions. This parameter is only one measure of the quality of the linear gradients [see *De Keyser*, 2008], but it can be seen that this remains low throughout the intervals containing FAC signatures (where there is significant current). As such, this parameter does not absolutely indicate accuracy, but, as a rule of thumb, a value of 30% has previously been used as a threshold indicator of reliable current estimates. The value is large and very noisy in the regions at either end of the interval where the current is zero and also shows a significant increase during the period of orbit crossover (04:11–04:12:30 UT). We therefore take this as a good indication of the overall quality of the estimates, although it only represents a measure of the nonlinear gradients, not the absolute error or the effect of time dependence. The further choice of four spacecraft from the five (time-shifted) positions allows us to probe the effects of both the different spatial coverage (shape of the four-spacecraft tetrahedron) achieved and time dependence through the different barycenter positions.

Two other events are shown in Figure 3 for longer intervals extending across the polar passes in each case. In the left plots, corresponding to the pass on the 28 April 2014, the profiles are remarkably matched, yet the increased amplitude of FACs caught by the four-spacecraft estimate is pronounced, particularly for the signature between 09:42 and 09:45 UT. Note that div**B** is again very small during the key intervals of FACs but shows low quality through the times adjacent to the orbit crossover and while the current density is very small. Similarly in the right plots, corresponding to the pass of the 4 May 2014, nearly all of the fine structure

of the FACs is reproduced in all estimates providing confidence that these features are well represented. Again, the amplitudes are caught best by the four-spacecraft estimates, and in this case the ABC configuration is also well matched to the other profiles. The values of div**B** are similar to the previous event with low values during the FACs.

4. Perpendicular Currents

In the case of the basic, two spacecraft method only the J_N current density component is obtained, so that any perpendicular currents are seen only through misalignment of the constellation plane to the background field. There may of course be errors introduced through lack of knowledge of the model field coordinates, but here we focus on the data-defined coordinates. Figure 4 shows the vector current density estimates obtained from the 4-point estimates for key intervals during the 22 April and 4 May passes and for two configuration choices. All components are in principle determined, so that $J_{||}$ and $J_{\perp}$ can be directly computed. The main FAC signatures in each event are indicated, and characteristic forms for the other components can be seen in each case. Clearly, as indicated in section 3, the FAC signatures agree in form between each method, although the amplitudes of the four-spacecraft curlometer are larger than the L2 parameter in some cases. We have shown a specific set of positions in Figure 4, based on time shifting the Swarm spacecraft A and C in order to remain as closely related to the L2 parameter as possible (as in section 3). The character of the signatures does change slightly with each choice of four spatial positions (selected from the five positions depicted on the orbit plots of Figures 2 and 3) but is most consistent for the optimum time shift giving the most regular configurations (in this case the value of div**B**/curl**B** is also most insensitive to the choice of configuration). Indeed, the form of the signatures overall remains recognizable, and in fact, the change in each component seen for the different estimates between the top and bottom plots is less than 0.2 μ Am^{-2} in the center of the main current signatures (which range in magnitude from about 2 to 4 μ Am^{-2}). This represents a maximum error in the estimates of around 10% due to changing the configuration. For the interval on the 22 April we have also marked the region where the estimates will be unreliable due to the orbit crossover.

In each case the perpendicular currents at either side of the FAC sheets are small but reach ~0.7 μ Am^{-2} and thus are significant. Furthermore, we have checked the effect of changing the time shift applied to the spacecraft positions and find that the perpendicular components remain significant, although smaller time shifts, of 5 or 10 s, severely distort the spatial configuration. For at least three of the signatures the perpendicular components show features which are consistent with the presence of perpendicular currents surrounding a FAC sheet [e.g., *Gjerloev and Hoffman*, 2002; *Liang and Liu*, 2007], i.e., reversals in the J_x and J_y components (SM coordinates) within the main FAC [see also *Ritter et al*., 2004; *Wang et al*., 2006]. These signatures will be analyzed in future work. Here we simply point out that the four-spacecraft technique can reveal perpendicular as well as parallel components. This is the first time these have been shown from direct measurements of the full vector current density at LEO, rather than as projections from single components [see *Shore et al*., 2013].

5. Conclusions

We have demonstrated here that the adoption of the principle of time-shifted measurements (in order to increase the number of spatial measurements of the magnetic field) can produce stable 2-, 3-, and 4-point estimates of the electrical current density. By applying the measurements only in the plane along the Swarm A/C orbit tracks, we obtain a set of estimates which are sensitive to the barycenter time and position. Here the component of the current density normal to the plane of the spacecraft positions is computed. This allows us to test for, and separate, effects which may be present over the time-shifted array used, i.e., temporal variations (by varying the value of the time shift) and degree of alignment of the computed component to the FACs. Increased stability of the signal measured from these alternative methods gives confidence in the quality of the estimates and increases the coverage possible with valid estimates. Indeed, we show that for the three- and four-spacecraft methods, the estimates are stable in intervals where the two-spacecraft method breaks down.

The four-spacecraft estimates are sensitive to the choice of spacecraft array and also to the choice of time shift, where the result depends on the degree to which the assumption of time independence over the measurement is satisfied. A number of different choices for the spacecraft positions were investigated by time shifting the Swarm ACB positions, and these can in principle also be used to probe the degree of stationarity

in the measurement of the current density by cross comparing estimates from the resulting spacecraft configurations (as in the case of the 3-point estimates). In general terms, the spatial estimate of current requires the currents to be stable on time scales equivalent to the effective convection time of the spacecraft array across the structure. These time scales can be compared to the time shifts used, and it was found here that the time shift which produces the most regular configuration results in the optimal estimates of current density. Moreover, for the regions containing FACs, where the main current component is nearly perpendicular to the Swarm AC orbits (by operational design), it is natural to time shift the Swarm A and C positions, and this in turn produces configurations which relate most closely to the L2 FAC data product. Nevertheless, in the region of study here, we find that the estimate of div**B**/curl**B** is generally small (high quality), where there is significant current and, once the time shift is optimized for tetrahedral shape, div**B**/curl**B** is relatively independent of the specific choice of four-spacecraft configuration (as selected from the five positions depicted in the left plot of Figure 1).

We have shown for the first time at low Earth orbit that a meaningful current density signal can be estimated for all components of the current density vector. This has two main consequences: the field parallel component can be directly computed rather than inferred from the projection of the normal component and the field perpendicular components can be estimated directly. The perpendicular components can reveal either residual Pederson currents or Hall currents associated with the FAC sheets, although at Swarm altitudes the Hall component is not expected. Future analysis will investigate the source of the perpendicular signal. One issue is that poor knowledge of the coordinates of the background model field and other error must be ruled out. Future work will also investigate the application of the magnetic gradient and curvature analysis [*Shen et al*., 2012b] to the time-shifted configurations.

Acknowledgments
We thank the ESA Swarm project for provision of the L1 data (https://earth.esa.int/web/guest/swarm/data-access) used here. This work is supported by the NSFC grants 41174141, 41431071, and 40904042; 973 program 2011CB811404; and by NERC grant NE/H004076/1. M.W.D. is partly supported by STFC in-house research grant. Y.Y.Y. is sponsored by China State Scholarship Fund (201404910456) to visit at RAL.

Michael Balikhin thanks Johan De Keyser and another reviewer for their assistance in evaluating this paper.

References

De Keyser, J. (2008), Least-squares multi-spacecraft gradient calculation with automatic error estimation, *Ann. Geophys.*, *26*, 3295–3316, doi:10.5194/angeo-26-3295-2008.

Dunlop, M. W., D. J. Southwood, K.-H. Glassmeier, and F. M. Neubauer (1988), Analysis of multipoint magnetometer data, *Adv. Space Res.*, *8*, 273.

Dunlop, M. W., A. Balogh, K.-H. Glassmeier, and the FGM team (2002), Four-point cluster application of magnetic field analysis tools: The curlometer, *J. Geophys. Res.*, *107*(A11), 1385, doi:10.1029/2001JA005088.

Dunlop, M. W., et al. (2015), Simultaneous field-aligned currents at Swarm and Cluster satellites, *Geophys. Res. Lett.*, *42*, 3683–3691, doi:10.1002/2015GL063738.

Friis-Christensen, E., H. Lühr, D. Knudsen, and R. Haagmans (2008), Swarm—An Earth observation mission investigating Geospace, *Adv. Space Res.*, *41*, 210–216, doi:10.1016/j.asr.2006.10.008.

Gjerloev, J. W., and R. A. Hoffman (2002), Currents in auroral substorms, *J. Geophys. Res.*, *107*(A8), 1163, doi:10.1029/2001JA000194.

Harvey, C. C. (1998), Spatial gradients and the volumetric tensor, in *Analysis Methods for Multi-Spacecraft Data*, edited by G. Paschmann and P. W. Daly, 307 pp., ESA Publ. Div., Noordwijk, Netherlands.

Liang, J., and W. W. Liu (2007), A MHD mechanism for the generation of the meridional current system during substorm expansion phase, *J. Geophys. Res.*, *112*, A09208, doi:10.1029/2007JA012303.

Lühr, H., J. Park, J. W. Gjerloev, J. Rauberg, I. Michaelis, J. M. G. Merayo, and P. Brauer (2015), Field-aligned currents' scale analysis performed with the Swarm constellation, *Geophys. Res. Lett.*, *42*, 1–8, doi:10.1002/2014GL062453.

Marchaudon, A., J.-C. Cerisier, M. W. Dunlop, F. Pitout, J.-M. Bosqued, and A. N. Fazakerley (2009), Shape, size, velocity and field-aligned currents of dayside plasma injections: A multi-altitude study, *Ann. Geophys.*, *27*, 1251–1266, doi:10.5194/angeo-27-1251-2009.

Olsen, N., H. Lühr, C. C. Finlay, T. J. Sabaka, I. Michaelis, J. Rauberg, and L. Tøffner-Clausen (2014), The CHAOS-4 geomagnetic field model, *Geophys. J. Int.*, *197*, 815–827, doi:10.1093/gji/ggu033.

Reigber, C., H. Lühr, and P. Schwintzer (2002), CHAMP mission status, *Adv. Space Res.*, *30*(2), 129–134.

Ritter, P., and H. Lühr (2006), Curl-B technique applied to Swarm constellation for determining field-aligned currents, *Earth Planets Space*, *58*, 463–476.

Ritter, P., H. Lühr, A. Viljanen, O. Amm, A. Pulkinnen, and I. Sillanpää (2004), Ionospheric currents estimated simultaneously from CHAMP satellite and IMAGE ground-based magnetic field measurements: A statistical study at auroral latitudes, *Ann. Geophys.*, *22*, 417–430.

Ritter, P., H. Lühr, and J. Rauberg (2013), Determining field-aligned currents with the Swarm constellation mission, *Earth Planets Space*, *65*, 1285–1294, doi:10.5047/eps.2013.09.006.

Robert, P., M. W. Dunlop, A. Roux, and G. Chanteur (1998), Accuracy of current density determination, in *Analysis Methods for Multispacecraft Data*, *ISSI Sci. Rep., SR-001*, Kluwer Acad, Noordwijk, Netherlands.

Shen, C., X. Li, M. Dunlop, Q. Q. Shi, Z. X. Liu, E. Lucek, and Z. Q. Chen (2007), Magnetic field rotation analysis and the applications, *J. Geophys. Res.*, *112*, A06211, doi:10.1029/2005JA011584.

Shen, C., Z. J. Rong, and M. Dunlop (2012a), Determining the full magnetic field gradient from two spacecraft measurements under special constraints, *J. Geophys. Res.*, *117*, A10217, doi:10.1029/2012JA018063.

Shen, C., et al. (2012b), Spatial gradients from irregular, multiple-point spacecraft configurations, *J. Geophys. Res.*, *117*, A11207, doi:10.1029/2012JA018075.

Shen, C., et al. (2014), Direct calculation of the ring current distribution and magnetic structure seen by Cluster during geomagnetic storms, *J. Geophys. Res. Space Physics*, *119*, 2458–2465, doi:10.1002/2013JA019460.

Shi, J. K., et al. (2010), South–north asymmetry of field-aligned currents in the magnetotail observed by Cluster, *J. Geophys. Res.*, *115*, A07228, doi:10.1029/2009JA014446.

Shi, J.-K., J. Guo, M. Dunlop, T. Zhang, Z. X. Liu, E. Lucek, A. Fazakereley, H. Reme, and I. Dandouras (2012), Inter-hemispheric asymmetry of the dependence of cusp location on dipole tilt: Cluster observations, *Ann. Geophys.*, *30*, 21–26, doi:10.5194/angeo-30-21-2012.

Shore, R. M., K. A. Whaler, S. Macmillan, C. Beggan, N. Olsen, T. Spain, and A. Aruliah (2013), Ionospheric midlatitude electric current density inferred from multiple magnetic satellites, *J. Geophys. Res. Space Physics*, *118*, 5813–5829, doi:10.1002/jgra.50491.

Vallat, C., I. Dandouras, M. Dunlop, A. Balogh, E. Lucek, G. K. Parks, M. Wilber, E. C. Roelof, G. Chanteur, and H. Rème (2005), First current density measurements in the ring current region using simultaneous multispacecraft Cluster-FGM data, *Ann. Geophys.*, *23*, 1849–1865.

Vogt, J., A. Albert, and O. Marghitu (2009), Analysis of three-spacecraft data using planar reciprocal vectors: Methodological framework and spatial gradient estimation, *Ann. Geophys.*, *27*, 3249–3273, doi:10.5194/angeo-27-3249-2009.

Wang, H., S. Y. Ma, H. Lühr, Z. X. Liu, Z. Y. Pu, C. P. Escoubet, H. U. Frey, H. Réme, and P. Ritter (2006), Global manifestations of a substorm onset observed by a multi-satellite and ground station network, *Ann. Geophys.*, *24*, 3491–3496, doi:10.5194/angeo-24-3491-2006.

Zhang, Q.-H., et al. (2011), The distribution of the ring current: Cluster observations, *Ann. Geophys.*, *29*, 1655–1662, doi:10.5194/angeo-29-1655-2011.